The Repeller Field debris mitigation approach for EUV sources

K. Takenoshita, C-S. Koay, M. Richardson
(Laser Plasma Laboratory, School of Optics-CREOL at University of Central Florida)

I.C.E. Turcu (JMAR Technologies Inc., San Diego, CA)

ABSTRACT

We describe studies of the debris produced from a high–repetition-rate laser plasma EUVL source based on the mass-limited target concept. In particular, we are developing mass-limited target designs based on complex targets containing tin. Comprehensive analysis of witness-plate detection techniques can reveal many interesting details of the interaction regime, and the impact of the debris. These techniques include Optical Microscopy, Scanning Electron Microscopy, Atomic Force Microscopy, X-ray Photoelectron Spectroscopy, Auger Electron Spectroscopy, and Auger Electron Microscopy. We also describe developments of the repeller field concept of debris inhibition. This technique uses electrostatic fields to reduce the flux of plasma ions impinging on the EUV collimating optics. Here, the first measurements of debris mitigation of a tin-doped target are described, and comparisons with earlier measurements of the impact of repeller fields on ion emission from a mass-limited water-droplet target are made.

1. INTRODUCTION

EUV light sources for advanced lithography need to meet several demanding requirements. These include the capability to provide high fluence of in-band EUV power at sufficiently high conversion efficiencies, and the need to operate stably at high-repetition-rates (~ 10-kHz) for long periods of time (> 6 months) without degrading the high reflective collimating mirrors used to collect the in-band emission for delivery to the lithographic imaging system. Mirror lifetime is a critical issue. Debris from the plasma source degrades the multi-layer mirror (MLM) reflectivity of the condenser optics. The overall lifetime of the combination of the plasma source and MLM optics depends mainly on how long the reflectivity of the first collimator mirror is maintained. It is a critical element in the system. This mirror is in direct line-of-sight of the source and sustains the full impact, not only of radiation outside the pass band of its coatings, but also of electrons, ions, neutral atoms and any particulate matter that originates directly from the target, or indirectly from other surfaces as a consequence of the source.

All these factors can degrade the mirror in different ways. For instance, particulate matter, depending on its state, and kinetic energy, can coat, chip and/or indent the surface of the mirror. Ions, on the other hand will, with sufficient energy, ablate or sputter the coating layers, while oxygen atoms will tend to oxidize the uppermost silicon layer of the mirror, reducing its reflectivity.

Our approach to maximizing the in-band conversion efficiency and minimizing the effects of debris is through the use of mass-limited targets. Here we define mass-limited as a target, whose mass is just sufficient for the target to be completely ionized during its interaction with a laser pulse. Ideally we then have a source that consists of the absolute minimum number of radiating ions necessary to produce the required power. Since 1992, we have been investigating the use of microscopic liquid droplets at high repetition-rate as limited-mass laser plasma targets[1-4]

We have previously made detailed lifetime studies of multilayer mirrors exposed to the long life effects of ions and particles from high repetition-rate (100 Hz) laser plasmas created from microscopic water droplet targets[5]. During this study, we developed several techniques that provide information on the progressive degradation of the mirror. We found, for instance, that Scanning Electron Microscopy (SEM) analysis of MLM's after this irradiation showed signs of sputtering by oxygen ions. In addition, if we slowed these ions down with a buffer gas, then X-ray

Emerging Lithographic Technologies VII, Roxann L. Engelstad, Editor,
Proceedings of SPIE Vol. 5037 (2003) © 2003 SPIE · 0277-786X/03/$15.00

Photoelectron Spectrometry (XPS) of the MLM's indicated oxidation of the mirror occurred. These studies also verified that MLM's sustained no detectable damage from particulate matter such as un-ionized chunks of material or even clusters when the water-droplet target was used as a source. This early work with water-droplet targets also led to the development of the repeller field concept of ion inhibition for debris mitigation[5].

In this paper, we describe the extension of these diagnostic techniques of debris impact measurement. In particular, we describe their application, for the first time, to studying debris from our mass-limited tin-doped laser plasma source. This microscopic source, not to be confused with other tin laser-plasma sources under development for EUV lithography[6-7] has a size approaching that which is needed for a mass-limited target--one that is completely ionized by the laser. Moreover, compared to these other tin target approaches, our target design contains only a small proportion (1% by atom) of tin. The focus of this paper is on the development of diagnostic techniques, principally witness-plate post-shot analysis techniques, that will both assess the level of debris, and also provide post-mortem information on the mechanisms giving rise to the debris.

A second topic in this paper describes initial testing of a new configuration of our repeller field concept for ionized debris inhibition. This double-cylinder repeller field configuration shows promise in stopping debris from the tin-doped micro target.

2. DEDICATED TEST FACILITIES FOR DEBRIS MEASUREMENT

The challenge and importance of precision measurements of the debris from high-repetition rate laser plasma targets has caused us to establish two laser plasma irradiation facilities dedicated to measurements of debris, the development of new debris analysis techniques, and the development of long life targets. These facilities are shown in Fig.1 and Fig. 2.

The experimental setup for debris measurement is shown in Fig. 1. The laser used for these debris measurements and mitigation tests is a commercial (Spectra-Physics GCR-190) 100-Hz, 300-mJ, 10 ns, Q-switched Nd:YAG laser (1064- nm). The laser beam is focused to a spot size of 80-µm diameter onto the micro-targets by using a 50-mm focal length positive lens. Typical intensities at the focal spot are in the order of 10^{11} W/cm^2. Glass plates and MLM are used as witness plates. They are placed close to the target, with a separation distance of 75-mm from the target. Experiments are carried out in a vacuum chamber at a pressure lower than 1-mTorr.

The experimental setup for debris mitigation is shown in Fig. 2. The same laser is used in this experiment. The current repeller field realization has the form of double-cylindrical structures. Stainless steel mesh with a transparency of 70% is used in the experiment. An array of witness plates can be placed around the source, with each plate located at the same distance from the source. The experiments are run at vacuum pressure of 500-mTorr in a chamber where the pressure can go lower than 1-mTorr. Section 4 will describe the repeller field configuration in greater details.

The mass-limited targets consist of a train of droplets produced from a dispenser capillary of 10-µm inner diameter. The laser beam is focused onto the target so that each laser pulse hits only one droplet target. Figure 3 shows a train of droplets whose droplet diameters are 30µm - 40µm and frequency 30 kHz – 300 kHz. The droplet has a mass of about 10-nanogram and it contains less than 1% of tin atoms.

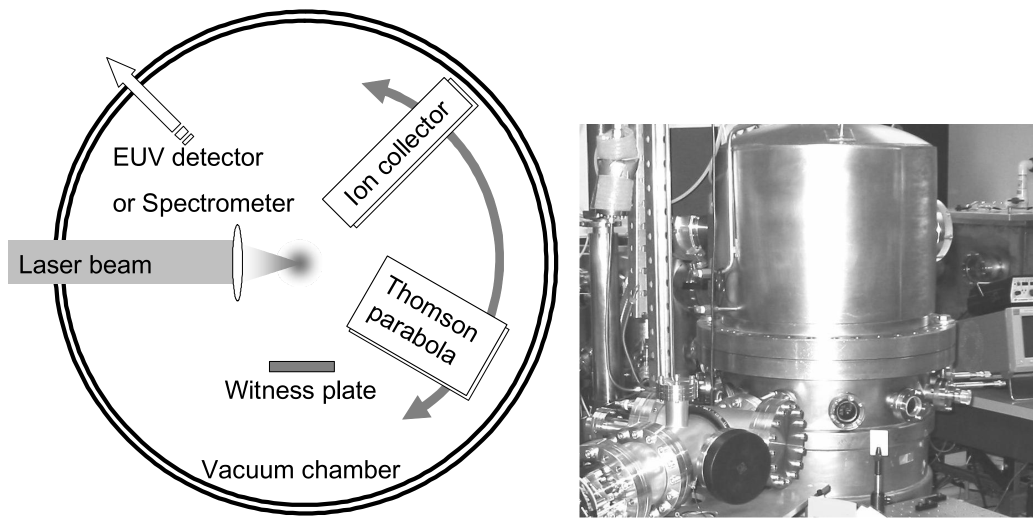

Figure 1: (a) experimental setup for debris measurement, (b) photograph of facility

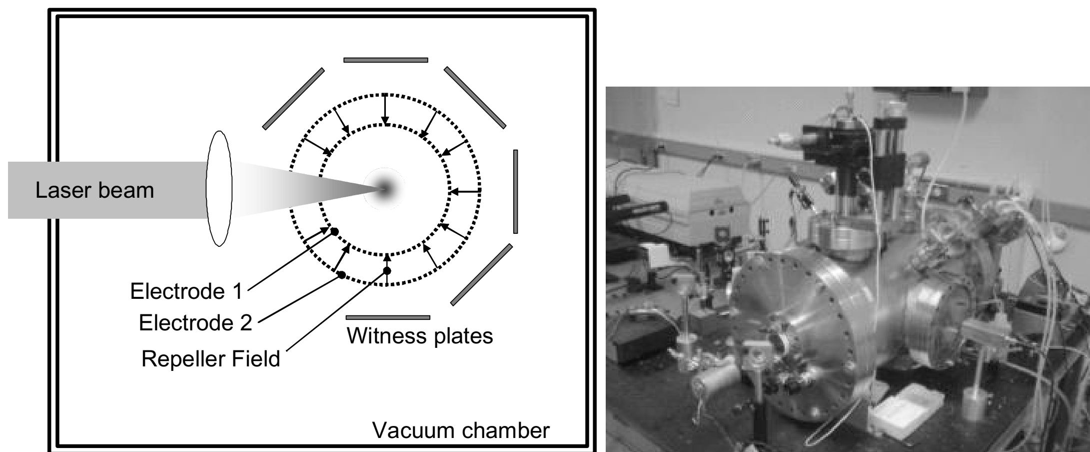

Figure 2: (a) experimental setup for debris mitigation, (b) photograph of facility

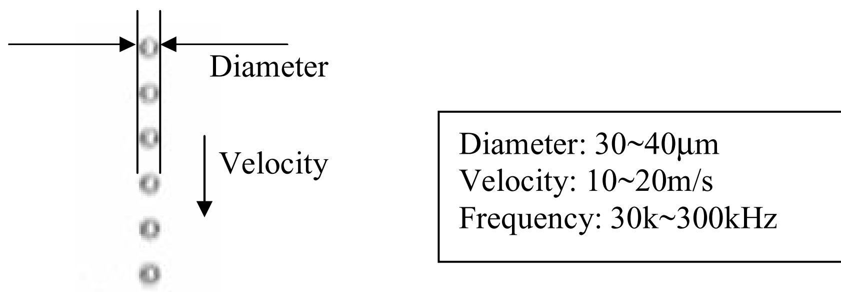

Figure 3: A train of droplet targets

3. DIAGNOSTIC METHODS FOR DEBRIS ANAYLSIS

Witness-plate post-shot analysis techniques as well as measurements of ions are used for debris analysis. The witness-plate post-shot analysis techniques can show direct result of the degradation caused by debris and the accumulated impact over a certain number of shots. Moreover, witness-plates can show the impacts caused by not only ions but also particulate matter which may not be charged at the time when the laser pulse and the target interact.

Glass plates (microscope slides) and MLMs are the witness-plates in the current experiments. The effects on the glass plates show mainly the impact of the matter emanated from the source that is deposited on the glass plates. The effects can be easily seen under an optical microscope. On the other hand, observations on the MLM witness-plates can reveal those microscopic impacts, such as sputtering or oxidation, of the surface layer by using a number of surface analysis techniques described below. MLM witness-plates, however, have an advantage for surface analysis over glass plates because a MLM sample can be analyzed with SEM and XPS subsequently on the same sample, whereas a glass plate sample cannot. Loss of conductivity following a coating process on the glass plate during the SEM analysis makes the glass plate unfeasible for the XPS as a subsequent test.

Measurement of ions can tell us about the ion velocity distributions and the species of ions. Charge collectors such as Faraday cup detectors and a Thomson parabola ion spectrometer are appropriate for such measurements. We are adding these techniques in the near future. Outlined below are initial results obtained from post-shot analysis of the witness-plates.

3.1 Particle analysis from Optical Microscopy (OM)

Optical Microscope (Nikon LABOPHOT-2) is used to observe macroscopic characteristics such as angular distribution. Glass plates were used as witness plates. They were placed in an array around the source, with each plate facing the source at different angles.

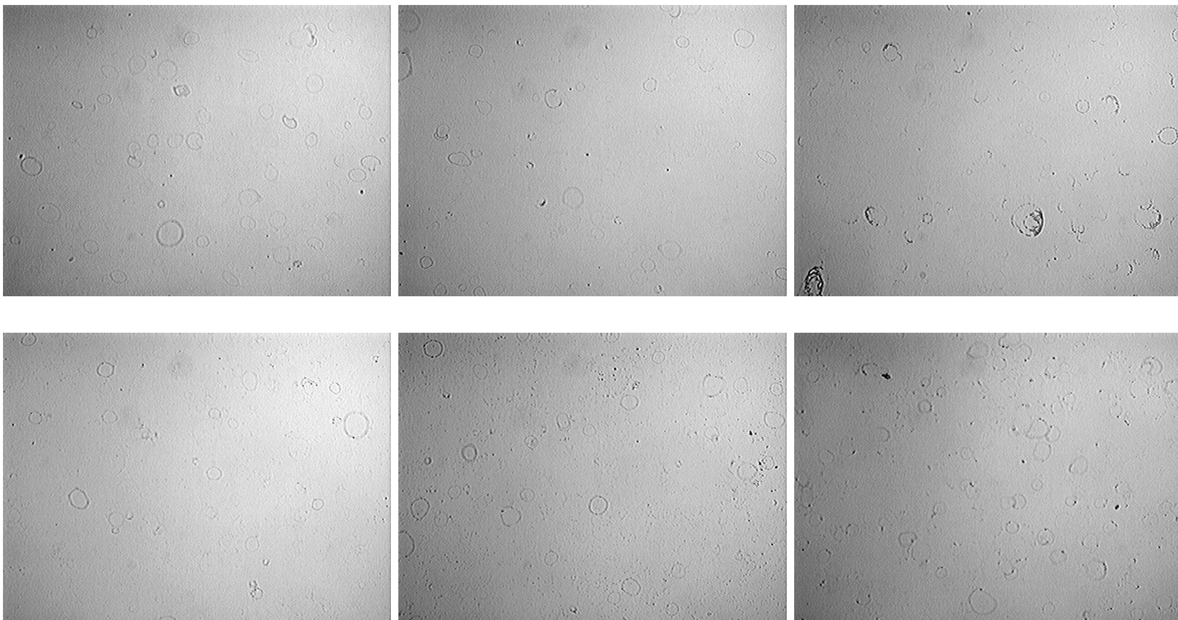

Figure 4: (a) X100 images of glass witness plate at 90 degrees from the laser beam's incident angle, (b) 135 degrees, (c) 180 degrees, (d) 225 degrees, (e) 270 degrees and (f) 315 degrees.

They were exposed to the laser plasma source for 1.4 x 10^5 laser shots when placed at a distance 30-mm away from the source. Figure 4 are images of the surface of each glass plate as seen through an X100 optical microscope. The amount of aerosol deposited on each plate is about the same and seems to be evenly distributed among all plates. This indicates that debris emanation occurs approximately evenly over the full 4π solid angle. The deposition elements on each plate comes in various sizes. Through OM observation, large deposits are easily seen while smaller size deposits are difficult to be seen. High magnification and resolution will be required for more refined observations.

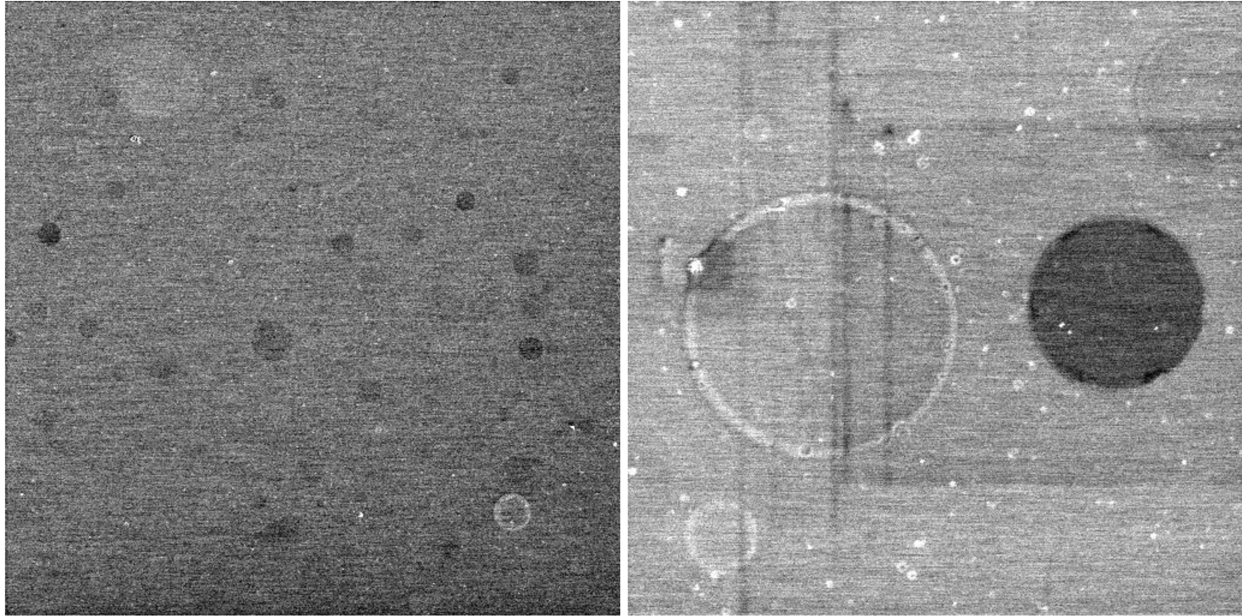

Figure 5 (a) SEM image of Tin deposition X1000, (b) SEM image X6000 magnification.

3.2 Scanning electron microscopy (SEM)

A SEM (JOEL JSM-6400F) is used to analyze the MLM witness-plates. Two different images of different magnifications are shown in Fig. 5. The MLM sample was exposed to the laser plasma source for 2.7 x 10^5 laser shots at a distance of 75-mm from the source. This sample was analyzed with all the diagnostic methods described in this section. Even though SEM images show the variation of the diameter of each deposit, the deposit thickness is unknown. Thinner deposits tend not to be seen in SEM images.

3.3 Atomic force microscopy (AFM)

An AFM (TA instrument μTA-2990) is used to determine the size of each deposit. Typical AFM images are shown in Fig. 6. An area of a 32.5–μm square was sampled with 400 resolution setting and sampling rate 32.5–μm/s. Some of the larger deposits appear in the form of rings. By analyzing the cross section profile of a deposit, the volume of the deposit can be calculated. The volume of the largest deposit is found to be 7 x 10^{-13} cm^3. Its mass is about 5 x 10^{-12} gram, which is less than 5 x 10^{-2}% of mass of a target. The minimum deposit thickness measured by AFM is about 2-nm. Identification of the material of the deposit is carried out by using other methods of diagnostics which will be described in the following section.

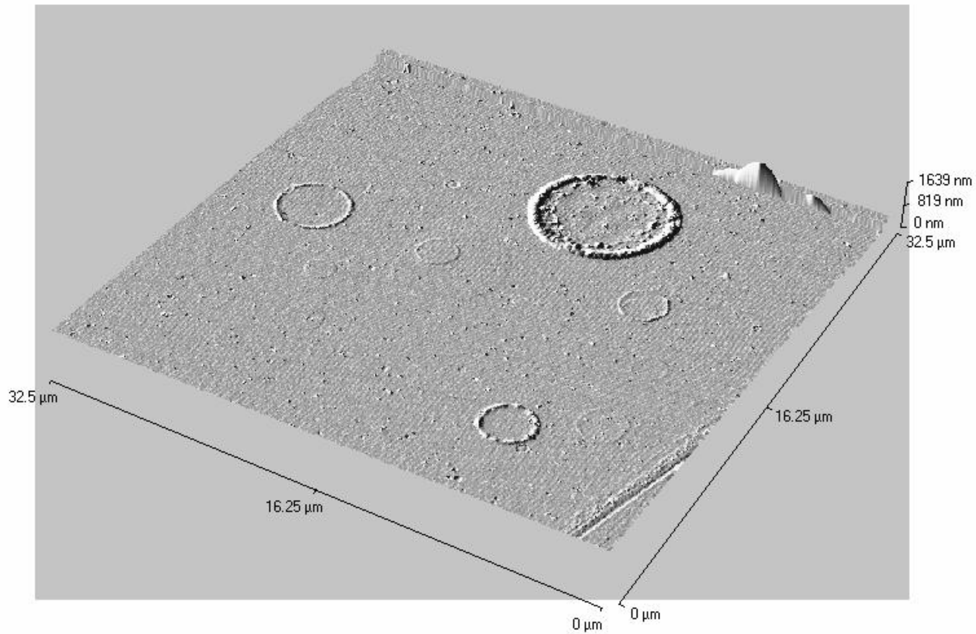

Figure 6: AFM image of tin deposition on a multilayer mirror.

3.4 X-ray photoelectron spectroscopy (XPS)

To identify the material of deposits, the XPS (Perkin-elmer PHI 5600) and AES (also described below) are used. In the XPS surface analysis, the spectroscopic measurement showed a result indicating tin material in the deposit.

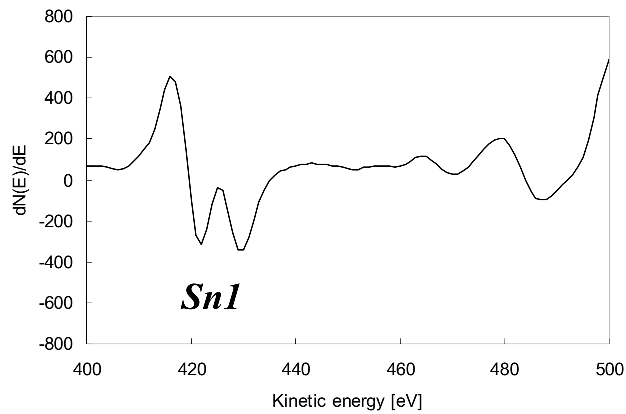

Figure 7: Tin signal measured by AES

3.5 Auger electron spectroscopy (AES)

The AES (Perkin-elmer PHI 600) was also used to identify the material of the deposits. A typical signal is shown in Fig. 7. Unlike the XPS, AES can detect material information of a deposit in a small area. By scanning the electron beam across the surface of interest, we obtained a map (image) of material distribution, described below.

3.6 Auger electron microscopy (AEM)

AEM analysis was done by using the same equipment as for the AES (Perkin-elmer PHI 600). Although an image obtained from the AEM is similar to that from the SEM, the AEM allows material mapping. Figure 8 shows an AEM image and a back-scattered image. Both images are taken from the same area of an MLM witness-plate surface. The back-scattered image shows the spatial distribution of high Z material, where the brighter spots are deposits of higher Z materials. The deposits shown in the AEM image completely overlapped the bright deposits on the back-scattered image. Since no signal of molybdenum was detected, all the deposits have to be tin.

By categorizing the deposit sizes and then counting the number of deposits, we estimated the total volume and mass of the deposition the MLM surface. Based on the AFM analysis, we can then calculate the volume of each deposit. The thickness of each deposit can be approximated as being proportional to its diameter so that the calculated volume fits to measured volume. From the results of the angular distribution of deposition, it is reasonable to assume that the sampled area of the MLM represents a spherical surface with a radius equaled to the source-mirror separation distance (75-mm). Hence, the total volume of tin deposited will be determined by multiplying the ratio of the surface area of the sphere to the MLM sampled area. Divide this number by the number of laser shots, the mass of deposited material on the MLM surface from a single target is obtained. The result shows that about 40% of the mass of the tin in a droplet target was accounted for in by the witness plate detector, on te assumption, veried above, that the emission was approximately isotropic.

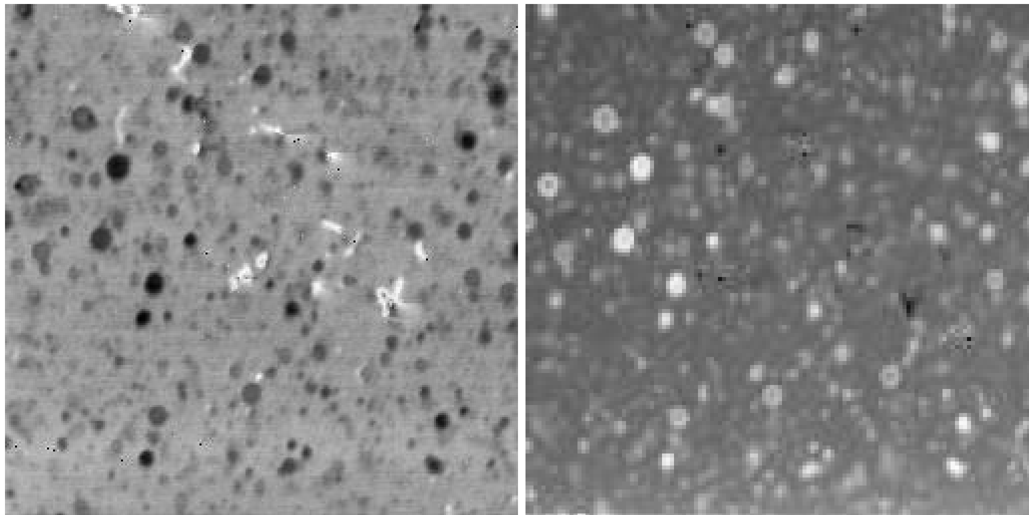

Figure 8: (a) AEM image 140µm X 140µm, (b) Back-scattered image (Same area)

4. A NEW REPELLER FIELD CONFIGURATION

The repeller field approach to debris mitigation was first applied to the water droplet target[5,8]. The authors found that ion sputtering on the surface of the MLM was the cause for the drop of reflectivity of the mirror with progressive exposure to the source. The installation of a repeller electrostatic field between the source and the MLM,reduced considerably the ion flow, resulting in extended life of the mirror, by at least a factor of ~ 10.

we are now testing a more advanced version of this reller field concept. The concept is shown in Fig. 9. Ions or charged particles will be repelled by the electric field established by the electrodes. Neutral clusters, however, are not affected by the field. They can pass through the field and deposit on the MLM surface.

The diameter of the inner electrode is 27-mm and its potential is maintained at –100 V. The outer electrode is 42-mm in diameter and it is at 300-V potential. MLM samples are placed 30-mm away from the plasma source and at a 90 degrees angle of from the laser beam incident. The mirrors were exposed to the plasma source for a total of $3x10^4$ laser shots.

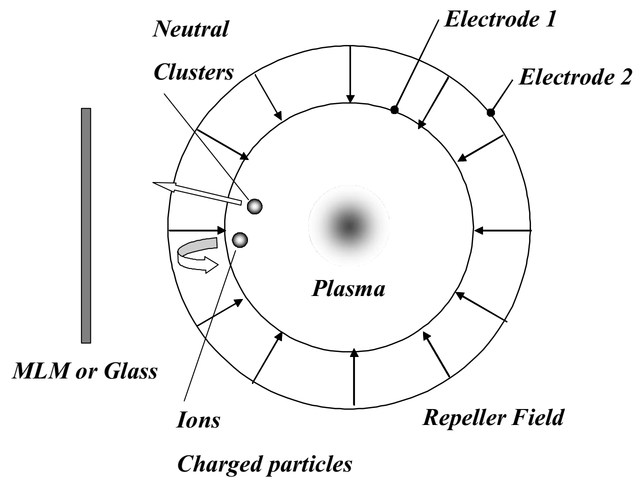

Figure 9: Concept of the repeller field

Initial results with this configuration are shown in Fig.9 This shows AEM back-scattered images of samples with and without the repeller field. . The size of each image is 500μm x 500μm.. The result shows significant reduction of tin deposits on the MLM surface when the repeller field was used. Further tests of this concept are in progress.

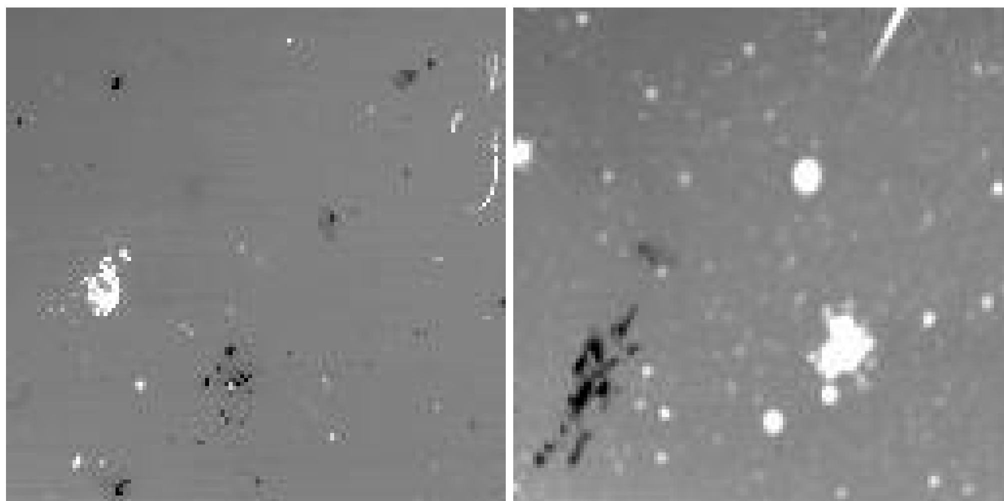

Figure 9: (a) AEM Back-scattered image with repeller field, (b) without repeller field.

CONCLUSION

Debris from laser plasmas produced from mass-limited targets is analyzed for the case of tin. Angular distribution of the debris was observed on glass witness-plates by optical microscopy. A small volume of tin deposition was observed on the multilayer mirror surface by SEM and AFM. The deposits are identified as tin by XPS and AES. The tin deposited on the MLM surface is quantified by a combination of AFM and AEM.techniques. Secondly, a new repeller field configuration is examined and shown to have a marked effect on the flow of debris from the target.

ACKNOWLEDGMENTS

The authors wish to acknowledge the technical assistance of colleagues with LPL at the School of Optics/CREOL, particularly Dr G Shimkaveg, Somsak Teerawattenasook, Joshua Duncan (CREOL). In addition they wish to thank David Attwood, and Eric Gullickson from Center for X-Ray Optics at LBL for the supply of multilayer mirrors This work was supported by a contract from JMAR Technologies Inc, and by the State of Florida.

REFERENCES

1. F. Jin, K. Gabel, M. Richardson, M. Kado, A.F. Vassiliev, and D. Salzmann, "Mass-limited laser plasma cryogenic target for 13 nm point x-ray sources for lithography," *Proc. SPIE*, vol. 2015, pp. 151-159, 1993
2. M. Richardson, D. Torres, C. DePriest, F. Jin, and G. Shimkaveg, "Mass-limited, debris-free laser plasma EUV source," *Optics Comm*., 145, pp. 109-112 (1998)
3. R.C. Constantinescu, J. Jonkers, P. Hegeman, and M. Visser, "A laser generated water plasma source for extreme-ultraviolet lithography and at wavelength interferometry," *Proc. SPIE*, vol. 4146, 101-112 (2000)
4. S. Dusterer, H. Schwoerer, W. Ziegler, C. Ziener, and R. Sauerbrey, "Optimization of EUV radiation yield from laser-produced plasma," *App. Phys. B*, 73, 693-698 (2001)
5. G. Shriever, M. Richardson & E. Turcu, The droplet laser plasma source for EUV lithography," *Proc. CLEO* 2000, p. 393-394 (2000),
6. I.C.E. Turcu, H. Rieger, A. Stone, J.H. Morris, H. Shields, M. C. Richardson, C. Keyser, K. Takenoshita, Chiew-seng Koay, "Overview of High Efficiency EUV Source Generated by Laser-Produced-Plasma" Extreme ultraviolet lithography (EUVL) source workshop, Oct. 14, 2002
7. T. Tomie, T. Aota, Y. Kurashima, N. Kandaka, H. Yashiro, K. Nishigori, I. Matsushima, and M. Komuro, "Study of a Cavity-confined Plasma as a Debris-Less and High Conversion Efficiency for EUV lithography," *Digest of Papers Microprocesses and Nanotechnology 2000*. 2000 International Microprocesses and Nanotechnology Conference (IEEE Cat. No.00EX387), Pages 284-285
8. M. Richardson and G. Schriever, US Patent 6,377,651, (2002)